

## MODELING AND ESTIMATION OF TRANSIENT CURRENT SIGNALS

Mohamed Nait Meziane\*, Philippe Ravier\*, Guy Lamarque\*, Karim Abed-Meraim\*,  
Jean-Charles Le Bunetel†, Yves Raingeaud†

\* PRISME Lab. - Université d'Orléans, 12 rue de Blois, 45067 Orléans, France

† GREMAN Lab. UMR 7347 CNRS-Université de Tours, 20 avenue Monge, 37200 Tours, France

### ABSTRACT

In this paper, we propose a nonstationary model for transient electrical current signals based on the physical behavior of electrical appliances during their turn-on. This model takes into account the nonstationarity of those transient signals and the special form of their envelope. We also propose an algorithm for the estimation of this model's parameters and we evaluate its performance on synthetic and real signals. The measured transient current signals actually reflect the physical phenomena appearing in the electrical appliances when turning on, and therefore, the model estimates of these transient current signals are useful for characterizing electrical appliances and can be helpful for distinguishing appliances in addition to the use of their steady-state power consumption.

**Index Terms**— Electrical current modeling, Turn-on transient, Nonstationary signals, Parameter estimation, NILM

### 1. INTRODUCTION

The work on Non-Intrusive Load Monitoring (NILM) systems have started in the late 80's with the work of Hart [1, 2] and is still gaining a rapidly growing interest [3, 4]. The idea of such systems is to monitor an electrical circuit, or load, (e.g. residential or commercial buildings) having a number of different appliances so that the system can estimate the number and nature of individual appliances (or group of appliances) and their respective energy consumption by analyzing the total load profile (current and voltage waveforms) measured at the main breaker level, hence, the non intrusive character of NILM systems.

In this paper, we present a study that was done in the context of NILM, where we analyze transient electrical signals in order to find parameters that can be used as characteristic ones to recognize and distinguish appliances from different classes or even recognize appliances of the same class. The transient behavior of electrical appliances is strongly influenced by the physical task that the appliance performs [5]. Recent studies show that turn-on transients improve appliance recognition

We would like to thank the Région Centre-Val de Loire (France) for their financial support of the project MDE-MAC3 (Contract n° 2012 00073640) under which this study was conducted.

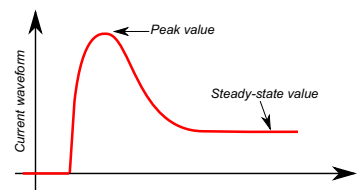


Fig. 1: Illustration for inrush current waveform.

accuracy [6]. The turn-on transient current of electrical appliances is usually called inrush current [7] and is characterized by a current waveform that has high values at the beginning of power consumption and decreasing values as time goes on (see Figure 1). This inrush current can appear for many reasons depending on the type of the considered appliance. For filament lamps, for example, it appears because of the filament resistance change related to its temperature change. Just as the current begins to flow, the temperature of the filament is low and so is its resistance which gives high current values. As the current continues to flow, the temperature of the filament and its resistance begin to grow high which decreases the current values. Other causes for this inrush current may be the charging of input capacitance in power converters or the energizing current of electric motors and transformers. In this paper, we call transient current signals, signals with a turn-on transient (we call hereafter transient-state part) plus a small portion of the steady-state part (called hereafter steady-state part). Along with the special form of the inrush current waveform, real signals can show a nonstationarity that comes from the time variations of signal parameters: frequency, phase, amplitude, etc. That's why we need to consider instantaneous parameters that take into account these variations in our model.

### 2. SIGNAL MODEL AND PARAMETER ESTIMATION ALGORITHM

#### 2.1. Signal model

Here we introduce the signal model proposed to represent transient current signals. We consider a noisy signal  $x(t) = s(t) + w(t)$  where  $s(t)$  is a noise-free signal and

$w(t)$  is a white Gaussian noise. This noise model is in agreement with the noise we found in our measurements (see section 3.2 for more details on measurements and transient signals' database). To represent inrush current  $s(t)$  we propose a model based on models using exponentially damped sinusoids [8]. The idea is based on the form of the inrush current waveform (see Figures 1) and expresses  $s(t)$  as a modulation of a sum-of-sinusoids signal  $S(t)$  by an envelope  $E(t)$ . For  $S(t)$ , we assume that its frequencies are fixed and are all odd order harmonics of the fundamental frequency  $f_1$  (50 Hz in our case) because of the odd half-wave symmetry we usually find in electrical signals (i.e. for a periodic signal  $g(t)$  with period  $T$ , we have  $g(t) = -g(t \pm T/2)$ ). If the frequencies are not fixed, but instead estimated, a slight estimation error will lead to an amplitude modulation modifying the signal's shape. Hence, for a better modeling, we exploit the information about the signal and its fundamental frequency and choose  $f_i = (1 + 2(i - 1))f_1$ ,  $i = 1, \dots, d$  ( $d$ : total number of frequencies). The envelope  $E(t)$  models the inrush current amplitude variation in the transient-state part of the signal whereas  $S(t)$  models the other related variations of the signal as a function of time, so that

$$s(t) = E(t)S(t), \quad (1)$$

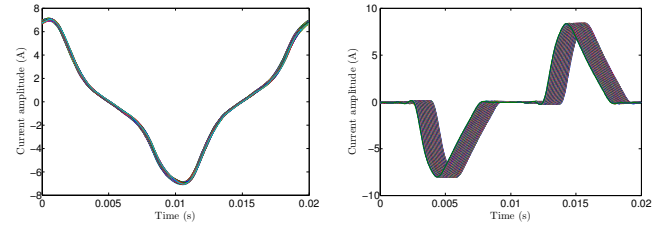
with

$$E(t) = A_0 e^{\mathbf{p}^T \mathbf{t}} + 1, \quad (2)$$

where  $A_0$  is a parameter adjusting initial amplitude and  $\mathbf{p} = [p_1, \dots, p_n]^T$  is a vector of  $n$  polynomial coefficients such that  $\mathbf{p}^T \mathbf{t}$  is a  $n^{\text{th}}$  order polynomial, with  $\mathbf{t} = [t, \dots, t^n]^T$  representing time vector. The "1" added to the envelope expression ensures that  $s(t) \xrightarrow{t \rightarrow +\infty} S(t)$  to obtain the steady-state part. To ensure that the envelope model  $E(t)$  converges, the condition we need to verify is  $\lim_{t \rightarrow +\infty} [E(t) - 1] = 0 \Rightarrow \lim_{t \rightarrow +\infty} \mathbf{p}^T \mathbf{t} = -\infty \Rightarrow p_n < 0$  (i.e. the last polynomial coefficient must be negative valued). The sum-of-sinusoids component  $S(t)$  is expressed as:

$$S(t) = \Re \left\{ \sum_{i=1}^d A_i(t) e^{j\varphi_i(t)} e^{j2\pi f_i t} \right\}, \quad (3)$$

where  $A_i(t)$ , and  $\varphi_i(t)$  ( $i = 1, \dots, d$ ) are slowly time-varying instantaneous amplitudes and phases of  $d$  complex exponentials and  $\Re$  stands for the real-part operator. The nonstationarity of signal parameters can be seen in Figure 2 where we have two examples of real signals taken from two different vacuum cleaners, one working at its maximum power consumption level (Figure 2a) and the other one working at its minimum power consumption level (Figure 2b). In this figure we took the steady-state part of the transient current signals and divided it into small windows of duration 20 ms each and then overlaid them. When the signal is stationary (Figure 2a) we get one repetitive elementary signal. In contrast, when



(a) Stationary real signal (b) Nonstationary real signal

**Fig. 2:** Illustration of nonstationarity in real signals.

the signal is nonstationary we get a group of elementary signals with varying parameters (the most apparent variation in Figure 2b is the phase parameter variation inducing a phase shift).

## 2.2. Parameter estimation algorithm

In this section, we present the proposed algorithm for the estimation of the parameters of the model defined in the previous section. The algorithm can be divided into four main parts. First a preprocessing step, then, the estimation of the sum-of-sinusoids signal  $S(t)$  followed by the estimation of  $E(t)$  and finally  $s(t)$  reconstruction. These parts are given in the steps below and explained later in the sequel. Note that estimated values are represented with a hat over the letter representing the considered variable.

### 1. Preprocessing:

- (a) Signal centering and filtering.
- (b) Null-current zones removal.

### 2. $S(t)$ estimation:

- (a) Choose  $d$  and fix  $f_i$ , ( $i = 1, \dots, d$ ).
- (b) Envelope  $E(t)$  detection: detected envelope is noted  $E_d(t)$ .
- (c) Normalize  $s(t)$  using  $E_d(t)$  to get  $s_{norm}(t)$ : this is to remove the envelope effect and keep only  $S(t)$  part.
- (d) Estimate  $A_i(t)$  and  $\varphi_i(t)$ , ( $i = 1, \dots, d$ ) from  $s_{norm}(t)$  and construct  $\hat{S}(t)$  using (3).

### 3. $E(t)$ estimation:

- (a) Choose  $n$  and compute  $\ln(E_d(t) - 1) = \ln(A_0) + \mathbf{p}^T \mathbf{t}$ .
- (b) Estimate parameters  $A_0$  and  $\mathbf{p}$  on transient-state part and construct  $\hat{E}(t)$  using (2).

### 4. $s(t)$ reconstruction: $\hat{s}(t) = \hat{E}(t)\hat{S}(t)$ .

The goal of the preprocessing step is mainly to remove any undesirable artifact found on the real signals. The filtering, for example, helps removing the undesirable impulsive switch noise [9] which is particularly apparent at high sampling frequencies. When an appliance doesn't consume power, we get a null-current zone in real signals which we want to remove during the preprocessing step. In the second step ( $S(t)$  es-

timation), we first choose the number of complex exponentials  $d$  (based on signal's frequency content and taking into account the filtering step), and then we fix the frequency values  $f_i = (1 + 2(i - 1))f_1$ ,  $i = 1, \dots, d$ . Envelope  $E(t)$  detection (step 2(b), where detected envelope is noted  $E_d(t)$ ) is done by first detecting the maxima (one maximum each fundamental period) of the transient current signal and then interpolating between them. It is worth noting that using a conventional approach such as finding the envelope using the analytic signal won't work because of the non suitable model in this case. In step 2(c), we normalize  $s(t)$  using  $E_d(t)$  to remove the envelope contribution, then, in step 2(d) we estimate  $A_i(t)$  and  $\varphi_i(t)$  using least squares (LS) technique. More precisely, these parameters being slowly time-varying, they can be considered as approximately constant over small time periods, typically, small data windows of duration [20 - 100] ms. Hence, for each data window, we use LS for the estimation of these amplitude and phase parameters. In the third step ( $E(t)$  estimation), we first have to choose  $n$ , the polynomial order. This is both a difficult and a critical choice to do and can significantly affect the performance of the algorithm which is highly dependent on the type of real signals we want to model. In this study, our choice of this parameter was based on empirical tests and we found that  $n = 3$  gave satisfactory estimation results for the real signals of our database. After this, in step 3(b), we estimate  $A_0$  and  $\mathbf{p}$  using a linear regression on the transient-state part and then we compute  $\hat{E}(t)$  to finally reconstruct  $\hat{s}(t)$  as  $\hat{s}(t) = \hat{E}(t)\hat{S}(t)$ .

### 3. RESULTS

In this section we evaluate the performance of the modeling and the parameter estimation algorithm on synthetic signals first and then on real signals using a transient electrical signals database we built.

#### 3.1. Evaluation using synthetic signals

We construct a synthetic signal (of eight seconds duration) based on signal model (1) to which we add white Gaussian noise at different Signal-to-Noise Ratio (SNR) levels. We choose  $d = 5$  frequencies, corresponding to the frequency vector  $f = [50, 150, 250, 350, 450]$ . To construct  $E(t)$  we choose  $A_0 = 1$  and  $\mathbf{p} = [-1, 0.5, -1]^T$ , so that we will have 3 polynomial coefficients to estimate. For  $S(t)$  we had to simulate the nonstationarity, so we chose the amplitude vector  $A = [1, 0.8, 0.4, 0.3, 0.1]$  and the phase vector  $\varphi = [0, 0, 0, 0, 0]$ , and we added some small random variations  $\Delta A$  and  $\Delta\varphi$  to them per periods of 1 s. The generated synthetic signal using these parameters is plotted in Figure 3. The model parameters were chosen so that the synthetic signal resembles as much as possible the measured real signals.

To evaluate the parameter estimation performance of our algorithm, we computed the Root-Mean-Square Errors (RM-

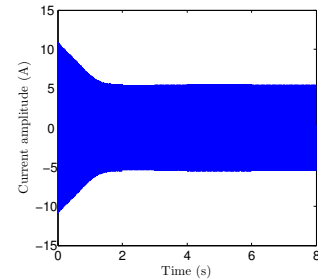
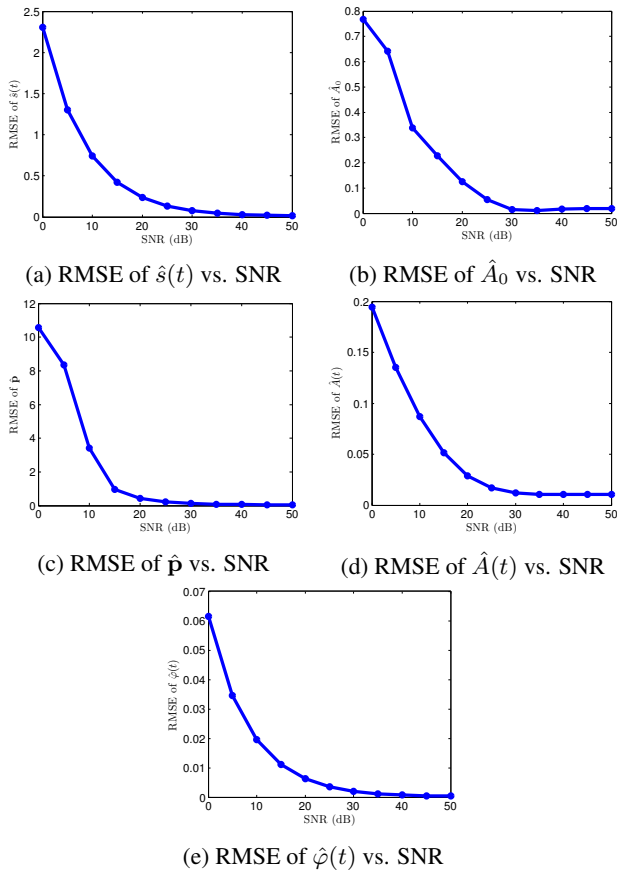


Fig. 3: Created synthetic signal without noise.

SEs) vs. different SNR values (0 to 50 dB) using 1000 Monte-Carlo iterations for each SNR level. The RMSEs were computed for the estimated signal  $\hat{s}(t)$  and parameter estimates  $\hat{A}_0$ ,  $\hat{\mathbf{p}}$ ,  $\hat{A}(t)$ , and  $\hat{\varphi}$ . Figure 4 shows the plots of these RMSEs. From these figures we clearly see that the errors decrease when the SNR value increases which is to be expected. Based on these simulations, we can say that for  $\text{SNR} \geq 25$  dB the RMSEs have relatively low values and the estimation performance of the algorithm can be qualified as good.

#### 3.2. Evaluation using our transient signals' database

To be able to study the considered transient signals, we are building a database of transient electrical signals taking measurements at a sampling rate of 100 kHz for different appliances. We are at the beginning of this database construction and to date we were able to make measurements for two types of appliances: vacuum cleaners and drills. We have 10 different vacuum cleaners (vacuum cleaner n°1 to vacuum cleaner n°10) and 8 different drills (drill n°1 to drill n°8). Most of these appliances have a variator that permits them to change their working power level. For such appliances we chose four levels for measurements: minimum (Min) and maximum (Max) power levels, and two intermediate levels (IL1, IL2). For each specific appliance type and level we made 50 measurements each of which we call instance. We have 1550 instances of vacuum cleaner signals and 1150 instances of drill signals which total 2700 instances in the database. These instances are 8.5 s long, beginning with a null-current zone (before consumption zone) and ending with a null-current zone (end of consumption zone) and between the two, a zone we call consumption zone. This latter is about 7 s long for vacuum cleaners and about 5 s long for drills. It is worth mentioning that not only transient current signals were measured but also corresponding transient voltage signals so that the computation of power consumption is possible. Figure 5 gives examples of four instances from the database, two instances from vacuum cleaner signals at "Min" and "Max" levels and two instances from drill signals also at "Min" and "Max" levels. Notice on the zoomed parts of the figure how signal shape changes from "Min" to "Max" levels and from appliance type to another. These changes are reflected in signal model (1)



**Fig. 4:** RMSEs computed for signal and parameters' estimation vs. SNR.

through the variations of its parameters.

To estimate the parameters of database signals using our proposed algorithm, we chose  $d = 5$  frequencies and a polynomial order  $n = 3$ . For the preprocessing we chose a low-pass filter of cut-off frequency equal to 1kHz and we used a power-based detector to remove null-current zones. To evaluate the parameter estimation algorithm performance on our database we applied it on 50 pairs (appliance type, appliance level) (e.g. pair (vacuum cleaner n°5, level "IL2")) each containing 50 instances of signals. The pairs numbered from 1 to 31 are vacuum cleaners and those numbered from 32 to 50 are drills. The obtained results are summarized in Figure 6 where we plot error bars (mean values with corresponding standard deviations) for the estimated parameters  $\hat{A}_0$ ,  $\hat{p}_1$ ,  $\hat{p}_2$ , and  $\hat{p}_3$  ( $\hat{A}_i(t)$  and  $\hat{\varphi}_i(t)$  are not presented here due to space limitation) of all 50 pairs. These error bars show that parameter estimates of vacuum cleaners are less variant than those of drills. Also,  $\hat{p}_3$  seems to be the least variant parameter which suggests its possible use as a characteristic parameter to represent an appliance class that includes vacuum cleaners and drills together (we can imagine for example a motor-driven appliances class). On the other hand, the range of  $\hat{A}_0$

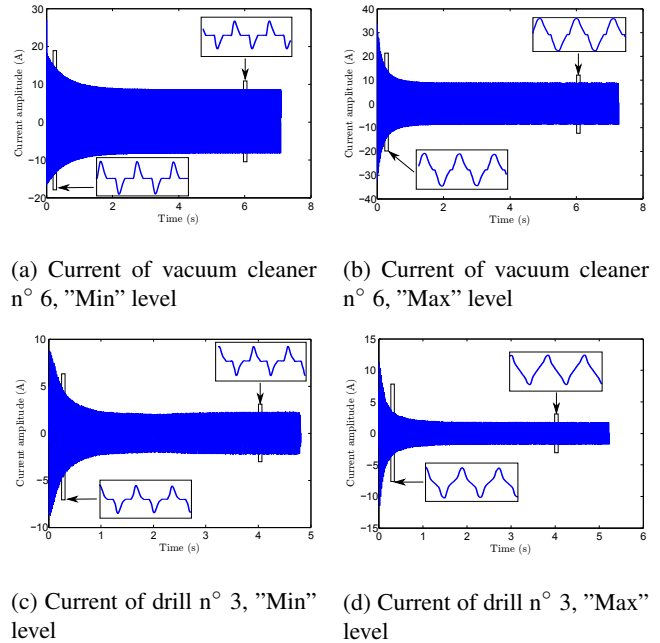


**Fig. 5:** Examples of transient current signals from database.

mean values of vacuum cleaners is different from the range of drill  $\hat{A}_0$  mean values which suggests that the use of  $\hat{A}_0$  as a characteristic parameter would better distinguish the vacuum cleaner class from the drill class. Figure 7 shows the computed steady-state active power (in Watts) for the appliances of the database (vacuum cleaners numbered from 1 to 10 and drills numbered from 11 to 18), with four power consumption levels represented for appliances that have a variator and one level for those who do not have one. We can see that the active power range of vacuum cleaners is higher than the active power range of drills. This difference in active power range is apparently reflected on the range of values of  $\hat{A}_0$  (Figure 6a). Note that drill n°7 (pairs n°46 to 49) is a drill press and is different than the other drills which are either hammer or rotary hammer drills. Also it has a nominal power consumption of 100 W whereas most of the other drills have nominal power consumption of 500 W. This explains the oddly different results with high estimate variance we see on Figures 6 for this specific drill. Drill n°1 (pairs n°32 to 35) also seems to give odd results which turn out to be due to the bad quality of this one (defective drill that gives very noisy signals).

Finally, we estimated the SNR for the real signals of our database, first, without filtering them (preprocessing step) and then using the filtering. The SNR is estimated as follows: first, we estimate the noise power  $\hat{\sigma}^2$  as the averaged value of the  $(L - n_s)$  least eigenvalues of the covariance matrix  $\mathbf{R}$  of  $\mathbf{s}(t) = [s(t), s(t-1), \dots, s(t-L)]^T$  where  $L$  is a window parameter satisfying  $L \gg n_s$ . The SNR is, then, evaluated as  $\frac{(\lambda_1 + \dots + \lambda_{n_s}) - n_s \hat{\sigma}^2}{\hat{\sigma}^2}$  where  $\lambda_1, \dots, \lambda_{n_s}$  are the prin-

	vacuum cleaner		drill	
	”Min”	”Max”	”Min”	”Max”
No filtering	26	33	23	25
Filtering	31	39	31	34

**Table 1:** Estimated mean SNR values (dB) for database signals at power consumption levels ”Min” and ”Max”

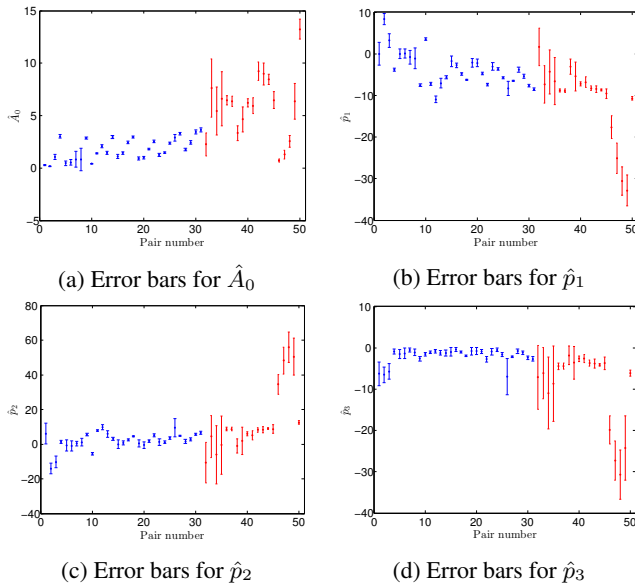


**Fig. 6:** Error bars for  $\hat{A}_0$ ,  $\hat{p}_1$ ,  $\hat{p}_2$ , and  $\hat{p}_3$ . Vacuum cleaners are represented in blue and drills in red.

cipal eigenvalues of  $\mathbf{R}$ . Table 1 gives mean values for the estimated SNR for vacuum cleaners and drills taken at their power consumption levels ”Min” and ”Max”.

We can, clearly, see the improvement of the SNR after using the filtering. Also, we see that most of these mean SNR values are greater than 25 dB which means that we are well within the SNR range where our estimation algorithm gives good results.

#### 4. CONCLUSION

In this paper we proposed a nonstationary model for transient electrical current signals’ representation along with an algorithm for its parameter estimation. We evaluated the estimation performance of this algorithm, using synthetic and real signals, and we showed that it gives good results within the proper range of SNR values ( $\geq 25$  dB). We also introduced our database of transient electrical signals and gave a brief description of it.

In future work, we intend to complete the database with more transient measurements from other types of appliances and use them to confirm the effectiveness of our model along with its corresponding parameter estimation algorithm.

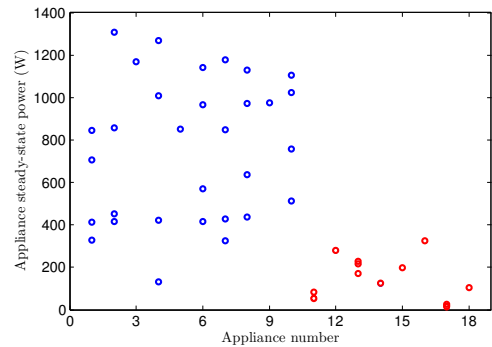


**Fig. 7:** Computed steady-state active power for database appliances. Vacuum cleaners in blue and drills in red.

A more detailed description of the database and related instrumentation may be considered in a future publication.

#### REFERENCES

- [1] G.W. Hart, ”Residential energy monitoring and computerized surveillance via utility power flows,” *Technology and Society Magazine, IEEE*, vol. 8, no. 2, 1989.
- [2] G.W. Hart, ”Nonintrusive appliance load monitoring,” *Proc. of the IEEE*, vol. 80, no. 12, pp. 1870–1891, 1992.
- [3] HH. Chang, LS. Lin, N. Chen, and WJ. Lee, ”Particle-swarm-optimization-based nonintrusive demand monitoring and load identification in smart meters,” *Industry Applications, IEEE Transactions on*, vol. 49, no. 5, pp. 2229–2236, 2013.
- [4] N. Batra, O. Parson, M. Berges, A. Singh, and A. Rogers, ”A comparison of non-intrusive load monitoring methods for commercial and residential buildings,” *CoRR*, vol. abs/1408.6595, 2014.
- [5] S.B. Leeb, S.R. Shaw, and J.L. Kirtley Jr, ”Transient event detection in spectral envelope estimates for nonintrusive load monitoring,” *Power Delivery, IEEE Transactions on*, vol. 10, no. 3, pp. 1200–1210, 1995.
- [6] HH. Chang, ”Non-intrusive demand monitoring and load identification for energy management systems based on transient feature analyses,” *Energies*, vol. 5, no. 11, pp. 4569–4589, 2012.
- [7] P.CY. Ling and A. Basak, ”Investigation of magnetizing inrush current in a single-phase transformer,” *Magnetics, IEEE Trans. on*, vol. 24, no. 6, pp. 3217–3222, 1988.
- [8] R. Kumaresan and D.W. Tufts, ”Estimating the parameters of exponentially damped sinusoids and pole-zero modeling in noise,” *Acoustics, Speech and Signal Processing, IEEE Trans. on*, vol. 30, no. 6, 1982.
- [9] E.K. Howell, ”How switches produce electrical noise,” *Electromagnetic Compatibility, IEEE Transactions on*, , no. 3, pp. 162–170, 1979.